Electric-Field-Induced Domain Evolution in Ferroelectric Ultrathin Films

Bo-Kuai Lai, I. Ponomareva, I. I. Naumov, I. Kornev, Huaxiang Fu, L. Bellaiche, and G. J. Salamo

Physics Department, University of Arkansas, Fayetteville, Arkansas 72701, USA

(Received 21 July 2005; revised manuscript received 9 February 2006; published 5 April 2006)

The electric-field-induced evolution of the recently discovered periodic 180° nanostripe domain structure is predicted in epitaxial $Pb(Zr_{0.5}Ti_{0.5})O_3$ ultrathin films from first principles. This evolution involves (1) the lateral growth of majority dipole domains at the expense of minority domains with the overall stripe periodicity remaining unchanged, (2) the creation of surface-avoiding *nanobubbles*, and (3) the formation of a single monodomain state. Analogies and differences (i) with ferroelectric thin films made of $BaTiO_3$ and (ii) with ferromagnetic thin films under magnetic field are discussed.

DOI: 10.1103/PhysRevLett.96.137602 PACS numbers: 77.22.Ej, 68.55.−a, 77.80.Bh, 77.84.Dy

Ferroelectric thin films are receiving an enormous amount of attention because of their technological promise in leading toward miniaturized and efficient devices [1]. An ongoing intensive fundamental effort has also been made to determine if (and understanding how) properties of these low-dimensional systems can differ from those of the corresponding three-dimensional bulk. As a result, recent studies revealed striking unusual features that are related to a particular characteristic of thin films, namely, their internal depolarizing fields. An example of such features is the prediction of a minimal critical thickness below which no ferroelectricity can exist [2]. Another example is the occurrence of an unusual dipole pattern [3,4], which consists of 180° stripe domains that, unlike domains in bulks, are periodic (and thus propagate throughout the *entire* material) with its periodicity being exceptionally small, that is, on the order of a few nanometers. Despite its obvious technological and fundamental importance, we are not aware of any study revealing how this peculiar stripe pattern evolves—and depends on the inherent parameters of the film—when applying the external factor that lies at the heart of many ferroelectric devices, namely, an external homogenous electric field. In particular, one may wonder if a phenomenon seen in ferromagnetic films under magnetic fields also occurs in ferroelectric films under electric fields, that is, the formation of so-called bubbles [5]. The discovery of such bubbles would make ferroelectric thin films of even broader interest, and would rise the questions of similitude or difference between the morphology, size, shape, and formation mechanism of bubbles in ferromagnetic versus ferroelectric thin films.

The aim of this Letter is to reveal from first principles, as well as to provide unprecedented detailed atomistic features of, the stripe domains' evolution in $Pb(Zr_{0.5}Ti_{0.5})O_3$ (PZT) ultrathin films under external electric fields. Such evolution does involve ferroelectric bubbles—as well as other features—that possess some striking differences (of technological promise) with respect to magnetic bubbles.

As in Ref. [3], the $Pb(Zr_{0.5}Ti_{0.5})O_3$ films are simulated to be grown along the [001] direction (which is chosen to be the z axis) and assumed to be Pb-O terminated at all surfaces. They are modeled by $40 \times 24 \times m$ supercells that are periodic along the x and y axes (which are chosen along the [100] and [010] pseudocubic directions, respectively) and where m is the number of finite (001) B layers along the *nonperiodic* z axis. The total energy of such supercells is used in Monte Carlo (MC) simulations, which typically run over 100 000 sweeps, and is written as

$$\varepsilon_{\text{tot}}(\{\boldsymbol{u}_i\},\{\sigma_i\},\{\boldsymbol{v}_i\},\eta) = \varepsilon_{\text{Heff}}(\{\boldsymbol{u}_i\},\{\sigma_i\},\{\boldsymbol{v}_i\},\eta) + \beta\Sigma_i\langle\boldsymbol{E}_{\text{dep}}\rangle\cdot Z^*\boldsymbol{u}_i - \Sigma_i\boldsymbol{E}\cdot Z^*\boldsymbol{u}_i, \quad (1)$$

where $\boldsymbol{u}_i$ is the local soft mode in the unit cell i of the film—whose product with the effective charge Z^* yields the local electrical dipole in this cell. The $\{\sigma_i\}$ arrangement characterizes the atomic configuration of the alloy [6]. The $\{\boldsymbol{v}_i\}$'s are the inhomogeneous strain-related variables inside these films [7]. η is the homogeneous strain tensor, which is particularly relevant to mechanical boundary conditions since *epitaxial* (001) films are associated with the freezing of three of the six components of η (in Voigt notation), which are $\eta_6 = 0$ and $\eta_1 = \eta_2 = \delta$, with δ being the value forcing the film to adopt the in-plane lattice constants of the chosen substrate [3,8,9]. $\varepsilon_{\text{Heff}}$ is the (alloy effective Hamiltonian) intrinsic energy of the ferroelectric film. Its expression and first-principles-derived parameters are those given in Refs. [6,10] for $Pb(Zr_{0.5}Ti_{0.5})O_3$ *bulk*, except for the dipole-dipole interactions for which we implemented the formula derived in Refs. [11,12] for thin film under ideal open-circuit (OC) conditions. Such electrical boundary conditions naturally lead to the existence of a *maximum* depolarizing field (to be denoted by $\langle\boldsymbol{E}_{\text{dep}}\rangle$) inside the film, when the dipoles point along the [001] direction. $\langle\boldsymbol{E}_{\text{dep}}\rangle$ is *exactly* derived at an atomistic level, following the procedure introduced in Ref. [11]. The second term of Eq. (1) mimics a *screening* of $\langle\boldsymbol{E}_{\text{dep}}\rangle$ thanks to the β parameter. More precisely, the residual depolarizing field, resulting from the combination of the first and second term of Eq. (1), has a magnitude equal to $(1-\beta)|\langle\boldsymbol{E}_{\text{dep}}\rangle|$. In other words, $\beta = 0$ corresponds to ideal OC conditions,

while an increase in β lowers the magnitude of the resulting depolarizing field, and $\beta = 1$ corresponds to ideal short-circuit conditions for which the depolarizing field has vanished. The third term of Eq. (1) represents the effect of a homogeneous electric field ($\boldsymbol{E}$) on the physical properties of the studied system [13]. In the present study, we consider only an electric field applied along the z axis and denote its magnitude as E_z.

Figure 1 shows the supercell average of the z-Cartesian component of the local modes ($\langle u_z \rangle = N^{-1}\Sigma_i u_{i,z}$, where N is the number of sites in the supercell) and of the *magnitude* of the local modes ($\langle u_M \rangle = N^{-1}\Sigma_i [{u_{i,x}}^2 + {u_{i,y}}^2 + {u_{i,z}}^2]^{1/2}$) as a function of E_z in 20 Å-thick ($m = 5$) ultrathin films. The temperature is 10 K and the misfit (compressive) strain is -2.65%. We chose here a realistic electrical boundary condition [2,4], which corresponds to an 81% screening of the maximum depolarizing field. Consistent with Refs. [3,4], the combination of a compressive epitaxial strain with a large enough residual depolarizing field leads to the formation of 180° stripe domains, when no external electric field is applied. Figure 2(a) displays such domains that adopt a periodicity of 8 unit cells (32 Å) for the considered 20 Å-thick ultrathin film. Such periodicity is unusually small with respect to the domain width of around 1000–10 000 Å observed in bulks [14–16] and is also in very good agreement with measurements and previous simulations [3,4,17] in films having comparable thickness. Inside each period, two stripe domains with (mostly) opposite out-of-plane dipoles—which we will refer to as "up" and "down" domains—alternate along the x axis. (Note that dipoles lying in plane can also be found at the top and bottom surfaces to further minimize the residual depolarizing field. The existence of such in-plane dipoles are likely the reason why omitting them in the analysis of the experimental data reported in Ref. [18] leads to incorrect results, such as the number of electrons for the Pb site being lower than the expected value.) The up and down domains can be considered as each having an equal width of 4 unit cells for $E_z = 0$, explaining why $\langle u_z \rangle$ vanishes while $\langle u_M \rangle$ is significantly larger than zero (see Fig. 1). Furthermore, Figs. 2(b)–2(f) provide atomistic detail on the evolution of the dipole patterns of the film, as given by the last snap shot of our MC simulations, when activating and increasing an applied electric field. Figure 3 provides complementary information on the number of supercell sites having a positive or negative z component of their dipoles, as well as on the average magnitude of such dipoles in the different (001) planes, as a function of E_z.

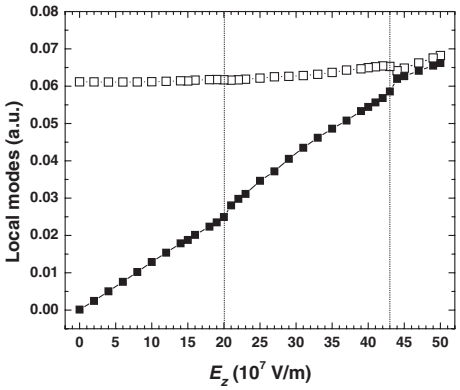

FIG. 1. Supercell average of the z-Cartesian component of the local modes, $\langle u_z \rangle$, and supercell average of the magnitude of the local modes, $\langle u_M \rangle$, as a function of the E_z, applied electric field along z axis for 20 Å-thick $Pb(Zr_{0.5}Ti_{0.5})O_3$ films under a compressive strain of -2.65%, a 81% screening of the maximum depolarizing field, and at $T = 10$ K. Open and solid symbols display $\langle u_M \rangle$ and $\langle u_z \rangle$, respectively. The supercell averages of the x- and y-Cartesian components of the local modes are essentially null and are not shown for clarity.

Figures 1 and 3 indicate that, when E_z increases from zero to 20×10^7 V/m, $\langle u_z \rangle$ linearly increases while $\langle u_M \rangle$ barely increases, because some sites rotate and flip their local dipoles towards E while very slightly increasing their magnitude. Comparing Figs. 2(a) and 2(b) reveals that such rotation and flip occur near the domain walls separating the up and down nanodomains. The up domains (i.e., for which the dipoles have a z component aligned along E thus grow laterally at the cost of the adjacent down (antiparallel) domains. Interestingly, the studied thin films still adopt a *periodic* stripe domain structure, with the overall periodicity remaining unchanged, during that lateral growth process [19]. Figures 2(b), 3(a), and 3(b) also indicate that, at the surfaces, the number of dipoles with in-plane components is reduced with respect to the $E_z = 0$ case in favor of dipoles having a positive z component. At the critical value $E_z = 20 \times 10^7$ V/m, the average width of the up and

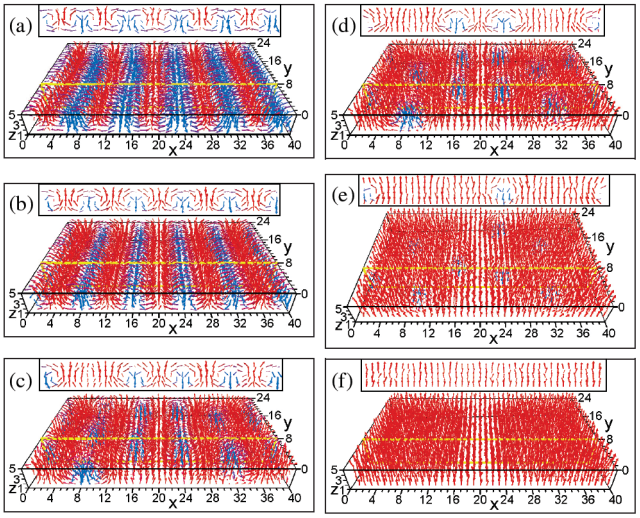

FIG. 2 (color). $T = 10$ K three-dimensional polarization patterns in (001) $Pb(Zr_{0.5}Ti_{0.5})O_3$ films under different E_z: stripe domains under (a) $E_z = 0$ and (b) $E_z = 18 \times 10^7$ V/m; bubble domains under (c) $E_z = 25 \times 10^7$, (d) $E_z = 31 \times 10^7$, and (e) $E_z = 43 \times 10^7$ V/m; monodomain under (f) $E_z = 47 \times 10^7$ V/m. The insets show the cross sections of a specific (x, z) plane (indicated by yellow lines). Red (blue) arrow characterizes local dipoles having a positive (negative) component along the z axis.

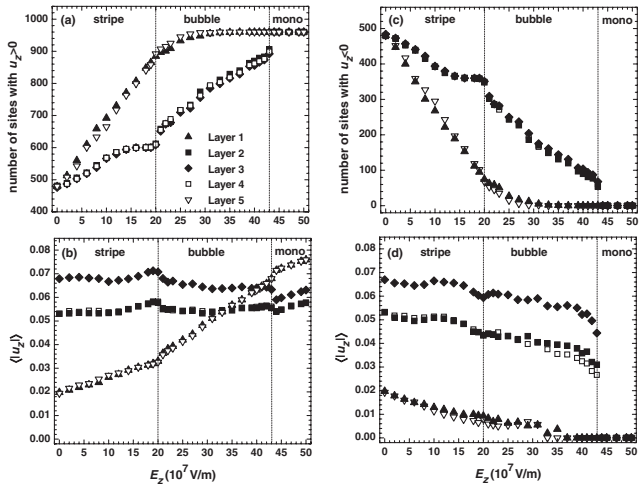

FIG. 3. (a) Number of sites with a positive z-Cartesian component of the local modes and (b) the corresponding $\langle|u_z|\rangle$ average magnitude of their z-Cartesian component of the local modes, as a function of E_z, in the different (001) layers at $T = 10$ K. (c) and (d) are the same as (a) and (b), respectively, but for a negative z-Cartesian component of the local modes. The layer index from the first layer (layer 1, which is a surface layer) to the last layer (layer 5, which is the other surface layer) are indicated by solid up-pointing triangles, solid squares, solid diamonds, open squares, and down-pointing open triangles, respectively.

down domains is numerically found to be 5 and 3 lattice constants, respectively.

As E_z keeps increasing above 20×10^7 V/m, a slight change in the slope of the $\langle u_z \rangle$ versus E_z curve happens (see Fig. 1), which is associated with the occurrence of the structural modification seen in Fig. 2(c): the smaller down domains become pinched along the y direction and three-dimensional nanobubbles (having dipoles still being antiparallel to the applied field) now emerge from this pinching. Such bubbles are *elongated* along the y direction and have a width of 3 lattice constants along the x axis, as direct consequences of the breaking of the previous down stripe domains along the y direction. As revealed by Figs. 3(a) and 3(c), the transition from stripe-to-bubble domains is accompanied by a sudden and discontinuous increase (respectively, decrease) of the number of sites belonging to the *inner* layers with positive (respectively, negative) z components for their dipoles. A *minimal* lateral (x) size of down domains of 3 lattice constants (12 Å), below which a periodic stripe domains structure cannot be stable anymore, thus exists in our 20 Å-thick films [see Figs. 2(b) and 2(c)]. Interestingly, when the down stripe domains reach such a minimal size, the dipole pattern first tends to rearrange itself while maintaining a periodic stripe domains structure before forming bubbles. Such rearrangement occurs when increasing the applied field from 15×10^7 to 20×10^7 V/m in the present case and essentially concerns the *surface layers*, where more dipoles acquire a positive and larger-in-magnitude z component, while inner layers do not flip or rotate their dipoles (see Fig. 3). As a result, bubbles do not (predominantly) ''touch the surface,'' once the transition from periodic up and down stripes to bubble domains occurs. Moreover, dipoles with (small) in-plane components exist around the bubbles in order to minimize the short-range energy costs associated with dipoles being antiparallel to the polarization.

Increasing even more $\boldsymbol{E}_z$ first leads to a *shrinking* of the bubbles along the y axis, and then to a decrease of the number of such bubbles once they reach a critical size of around 3 lattice constants along this y axis; see Figs. 2(c)–2(e). The lateral size of the bubbles along the x axis remains equal to 3-lattice constants during these processes. When the applied electric field becomes as large as 43×10^7 V/m, the bubbles disappear in favor of a monodomain state [see Fig. 2(f)]. Increasing E_z further results in the elongation of the dipoles along z within the monodomain, as indicated by the increase of both $\langle u_z \rangle$ and $\langle u_M \rangle$ seen in Fig. 1.

Moreover, we also *decreased* E_z from 50×10^7 V/m to zero, and found that the resulting domain evolution sequence is simply the reversal process of the one we just described when *increasing* the applied electric field. We also investigated the effects of the residual depolarizing field's magnitude, misfit strain, and film thickness on the domain evolution. For instance, solely decreasing the β screening coefficient from 81% to 41% does not qualitatively affect the domain evolution described above but rather increases ''only'' the critical applied fields (which are now equal to 120×10^7 and 320×10^7 V/m at the stripe-to-bubble and bubble-to-monodomain transitions, respectively, versus 20×10^7 and 43×10^7 V/m before). This increase occurs because a smaller β yields a larger depolarizing field, and that larger depolarizing field favors the formation of up and down domains (to fight against it) over bubbles and even more over monodomains. Similarly, an increase of the film thickness from 20 to 36 Å, while maintaining $\beta = 0.81$ and a misfit strain of -2.65%, leads to an increase of these critical fields (now around 74×10^7 and 90×10^7 V/m at the stripe-to-bubble and bubble-to-monodomain transitions, respectively). This is likely due to the fact that thicker films under a residual depolarizing field and a compressive strain have a larger initial (i.e., corresponding to $E_z = 0$) stripe domains period [4,17]. It thus takes larger applied fields to move the domain walls until reaching the minimal lateral x width of the down domains, which we found to be around 8–12 Å, independently of the film thickness. Note also that the range of electric field associated with nanobubbles becomes smaller when increasing the thickness. This is caused by the fact that the bubbles are laterally (i.e., along the x axis) farther away from each other, because of the initially larger stripe period. We also found that increasing the magnitude of the compressive strain slightly decreases the critical fields; e.g., a misfit strain of -3.0% yields stripe-to-bubble and bubble-to-monodomain transitions at 18×10^7 and 40×10^7 V/m, respectively (to be compared to 20×10^7 and 43×10^7 V/m for the misfit strain of -2.65%), because higher compressive strain favors elastic-related energies

(that prefer monodomains and then bubbles in this order [5] rather than stripe domains) over the depolarizing energy (that is, the lowest in stripes and the highest in monodomains and in between for bubbles).

Let us now compare our results for [001] PZT films under an external electric field with those obtained for [001] $BaTiO_3$ thin films (not shown here). We found that these latter low-dimensional systems also adopt, when no external field is applied, a 34 Å-periodic stripe structure (with up and down dipoles along the z axis), for a thickness of 20 Å, a screening coefficient β of 0.80, and a misfit compressive strain of -2.22%. However, unlike in PZT films and as consistent with Ref. [20], these stripes alternate along the [110] direction rather than the [100] direction (because of some short-range interactions). Despite this difference in morphology, the $BaTiO_3$ thin films behave in a same qualitative fashion than the PZT films when progressively increasing E_z, in the sense that the following three general field regimes exist: (i) the down and up nanostripe structure first evolves such as to yield a nonzero spontaneous polarization with the stripe structure's periodicity remaining unchanged; (ii) nanobubbles are then created when the width of the down domains becomes close to 11 Å in average (the up domains being 23 Å wide) and then contract; (iii) the bubbles then become unstable resulting in the creation of a monodomain whose dipoles elongate along the z axis when further increasing E_z. We also found that the dependencies of the field regimes on thickness and depolarizing field is qualitatively the same between $BaTiO_3$ and PZT thin films. On the other hand, increasing the magnitude of the compressive strain slightly increases the critical fields in $BaTiO_3$ films, rather than slightly decreasing them as in PZT thin films. This difference is likely due to the fact that flipping dipoles in the ''soft'' PZT material is easier to accomplish than in the ''harder'' $BaTiO_3$ compound.

Finally, we wish to draw parallels and differences between our predictions for ferroelectric films under an applied electric field (displayed in Figs. 1–3) and known features of ferromagnetic thin films subject to an external magnetic field. For that, it is important to realize that modification of periodic stripes, and transitions from stripes-to-bubbles domains and bubbles-to-monodomains are also known to occur in ferromagnetic films under magnetic fields [5]. However, it is commonly believed that the lateral growth of up domains at the expense of down domains is accompanied by a modification of the stripes' *periodicity* in magnetic films under magnetic fields, while our results on ferroelectric films under electric field show otherwise [5]. This may be due to the fact that the stripe periods are an order of magnitude smaller in ferroelectric films with respect to ferromagnetic films [21]. Moreover, the shape of ferroelectric bubbles is elliptical rather than spherical, as commonly assumed in magnetic bubbles [5]. Furthermore, our ferroelectric bubbles avoid the surfaces, which is in contrast with a common belief [22] (based on the presence of defects at the surfaces) and which can be due to the fact that our thin films are defect free. Finally, the ferroelectric bubbles (which have a lateral width of 12 Å) are far smaller than the ferromagnetic bubbles (which are at least 500 Å in diameter) [23]. The ferroelectric bubbles domains could thus deliver the promises that the magnetic bubbles have never fulfilled for memory or logic devices applications, because of their relatively large diameter and low operation speed [23].

In summary, we have revealed—and provided detailed atomistic insight of—the domain evolution of epitaxial ultrathin films under an applied electric field. We hope that our predictions and, in particular, the formation of bubbles will be confirmed soon and will lead to further investigations on the fascinating topic of domain structures in low-dimensional ferroelectrics and ferromagnets.

This work is supported by ONR Grants No. N00014-01-1-0365, No. N00014-04-1-0413, and No. 00014-01-1-0600, by DOE Grant No. DE-FG02-05ER46188, and by NSF Grants No. DMR-0404335 and No. DMR-9983678.

[1] J. F. Scott, *Ferroelectric Memories* (Springer-Verlag, Berlin, 2000).
[2] J. Junquera and P. Ghosez, Nature (London) **422**, 506 (2003).
[3] I. Kornev, H. Fu, and L. Bellaiche, Phys. Rev. Lett. **93**, 196104 (2004).
[4] S. K. Streiffer *et al.*, Phys. Rev. Lett. **89**, 067601 (2002).
[5] A. Hubert and R. Schafer, *Magnetic Domains: The Analysis of Magnetic Microstructures* (Springer, Berlin, 1998).
[6] L. Bellaiche, A. Garcia, and D. Vanderbilt, Phys. Rev. Lett. **84**, 5427 (2000).
[7] W. Zhong, D. Vanderbilt, and K. M. Rabe, Phys. Rev. Lett. **73**, 1861 (1994).
[8] Y. L. Li *et al.*, Appl. Phys. Lett. **81**, 427 (2002).
[9] N. A. Pertsev *et al.*, Phys. Rev. B **67**, 054107 (2003).
[10] L. Bellaiche, A. Garcia, and D. Vanderbilt, Ferroelectrics **266**, 41 (2002).
[11] I. Ponomareva *et al.*, Phys. Rev. B **72**, 140102 (2005).
[12] I. I. Naumov and H. Fu, cond-mat/0505497.
[13] L. Bellaiche, A. Garcia, and D. Vanderbilt, Phys. Rev. B **64**, 060103(R) (2001).
[14] G. Arlt and P. Sasko, J. Appl. Phys. **51**, 4956 (1980).
[15] J. L. Giocondi and G. S. Rohrer, Mater. Res. Soc. Symp. Proc. **654**, AA7.4.1-10 (2001).
[16] W. J. Merz, Phys. Rev. **95**, 690 (1954).
[17] Z. Wu *et al.*, Phys. Rev. B **70**, 104108 (2004).
[18] D. D. Fong *et al.*, Phys. Rev. B **71**, 144112 (2005).
[19] Note that we used different supercell sizes to confirm that the overall stripe periodicity is indeed unchanged.
[20] S. Tinte and M. G. Stachiotti, Phys. Rev. B **64**, 235403 (2001).
[21] M. Liebmann *et al.*, Phys. Rev. B **71**, 104431 (2005).
[22] V. Y. Shur and E. L. Rumyantsev, Ferroelectrics **191**, 319 (1997).
[23] T. H. O'Dell, Rep. Prog. Phys. **49**, 589 (1986).